Materials Chemistry and Physics 125 (2011) 326–333

Contents lists available at ScienceDirect

Materials Chemistry and Physics

journal homepage: www.elsevier.com/locate/matchemphys

Low temperature combustion synthesis of $Co_xMg_{1-x}Al_2O_4$ nano pigments using oxalyldihydrazide as a fuel

I.S. Ahmed*, S.A. Shama, H.A. Dessouki, A.A. Ali

Chemistry Department, Faculty of Science, 25-eloumda, Benha University, Benha, Egypt

ARTICLE INFO

Article history:
Received 28 January 2010
Received in revised form 7 October 2010
Accepted 7 November 2010

Keywords:
Cobalt-based ceramic pigments
Oxalyldihydrazide
Low temperature combustion synthesis
Calcination temperature

ABSTRACT

Oxalyldihydrazide as a fuel was used to prepare new nano size blue refractory ceramic pigments $MgAl_2O_4$: xCo^{2+} ($0.00 \leq x \leq 0.10$) using low temperature combustion synthesis (LCS) method. The synthesized and calcined powders were characterized by Fourier transform infra red (FTIR) spectrometry, electronic spectra, thermogravimetry, differential thermogravimetry, differential thermal analysis, X-ray diffraction (XRD) analysis, and transmission electron microscopy (TEM). Also, the color measurements of nano pigments are studied by diffuse reflectance spectroscopy (DRS) using CIE-$L^*a^*b^*$ parameter method. The FTIR spectra show frequency bands in range the 422–700 cm^{-1} correspond to metal oxygen bonds through vibrations for the spinel structure compound. The average particle size of prepared samples as determined from XRD and TEM was 30 nm at 1100 °C. Also, the results revealed the varying bulk density, particle size, shape and color with different calcination times and temperatures.

© 2010 Elsevier B.V. All rights reserved.

1. Introduction

Nano-pigments are inorganic or organic materials, insoluble, chemically and physically inert into the substrate or binders with particle size less than 100 nm [1,2]. The ceramic pigments with particle size in the nano scale have massive potential market, because of their high surface area, which assures higher surface coverage, higher number reflectance points and hence improved scattering. Ceramic pigments are basically a white or colored material, having high thermal stability and chemical resistance in order to be used at high temperature [3–5]. Recently the development of a new ceramic pigment has fostered the research and application of pigments stable over 1200 °C. Ceramic pigments based on oxides, spinels, aluminates are prepared with blends of oxides as starting mixtures with proper particle size distribution of powders, also employing additions of salt like halides and borates that have mineralizing function [6,7]. Recently, attempts to synthesize ceramic materials at low temperatures have been carried out by several solution techniques such as sol–gel [8–11], co-precipitation [12], hydrothermal [13,14], alkoxide hydrolysis [15–17], Penchini method [18,19], and low combustion method [20–25]. White $MgAl_2O_4$ [26] and red $Ce_{1-x}Pr_xO_{2-\delta}$ [27] pigment powders are prepared by auto-ignition route (combustion method). Light or dark beige, brown and black ceramic powders $Co_xZn_{7-x}Sb_2O_{12}$ [28], light reddish-yellow ceramic pigment $MgFe_2O_4$ [29], brown pigment $BaFe_2O_4$ and red ceramic pigments $CaFe_2O_4$ [30,31] were prepared using the polymeric precursor method. Co_2SiO_4 (olivine), $(Co,Zn)_2SiO_4$ (willemite), $CoAl_2O_4$ (spinel), Co_2SnO_4, $(Co,Zn)Al_2O_4$, $Co(Al,Cr)_3O_4$, $(Co,Mg)Al_2O_4$ and $(Co,Zn)TiO_3$ [32,33] are used as blue pigments. But cobalt is scarce and expensive, thus increasing the production costs of cobalt-based ceramic pigments. Moreover, serious environmental problems may occur from the manufacturing process of Co-based ceramic pigments [34,35]. A new application of the spinels as ceramic pigments has been explored, owing to their high mechanical resistance, high thermal stability, low temperature sinterability and the easy incorporation of chromophore ions into the spinel lattice, allowing for different types of doping, thus producing ceramic pigments with different colors [36]. Blue pigments are widely used in industry to bring color to plastics, paints, fibers, papers, rubbers, glass, cement, glazes, ceramics, and porcelain enamels [37]. The synthesis route is very important to determine the final properties of nano inorganic pigments such as coloring agent, particle size, resistance to acids and alkaline.

The present paper aims at synthesizing ceramic blue pigments from the system $Co_xMg_{1-x}Al_2O_4$ spinel nano ceramic pigments using low temperature combustion method using oxalyldihydrazide fuel. The $Co_xMg_{1-x}Al_2O_4$ system allows for a reduction in the production costs and also for minimizing the environmental damage, as the amount of cobalt is reduced.

2. Experimental

2.1. Materials and reagents

All the starting chemicals used in this study are of pure grade: aluminum chloride hexahydrate (Aldrich), magnesium chloride hexahydrate (Aldrich),

---

* Corresponding author. Tel.: +20 122408034.
E-mail addresses: isahmed2010@gmail.com, isahmed61@gmail.com (I.S. Ahmed).

0254-0584/$ – see front matter © 2010 Elsevier B.V. All rights reserved.
doi:10.1016/j.matchemphys.2010.11.009

cobalt(II) chloride hexahydrate (Aldrich), sodium carbonate (Merck), ethyl oxalate (Aldrich), nitric acid, 65% (Merck) and hydrazine hydrate, 99.9% (Merck).

2.2. Synthesis of oxalyldihydrazide (ODH) as a fuel

The oxalyldihydrazide (ODH) has the large reducing power and produces the large volume of gas (7 mol mol^{-1} of ODH). Oxalyldihydrazide (ODH) used as a fuel was prepared by the drop wise addition of one mole ethyl oxalate to two mole of hydrazine hydrate (99.9%) was cooled in an ice bath according to the following equation [38].

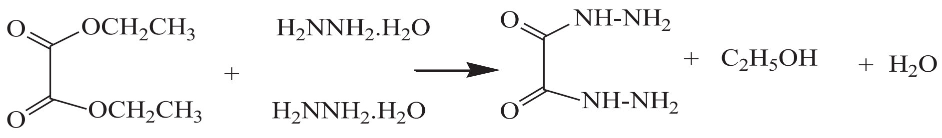

2.3. Synthesis of $Co_xMg_{1-x}Al_2O_4$ nano ceramic pigments

Nano ceramic pigments $Co_xMg_{1-x}Al_2O_4$ ($0.00 \le x \le 0.10$) were prepared using metal salts and then dissolved in distilled water, precipitated with sodium carbonate, good washing and drying. The above mixture was dissolved in nitric acid, heated to become clear solution, cooled to room temperature, and then oxalyldihydrazide was added as a complexion agent. The resulting solution was heated to 80 °C for 3 h with vigorous stirring until clear gel solution appeared, transferred into furnace that was preheated to 500 °C. The precipitate initially started to swell and filled the beaker, producing a foamy precursor, this foam consisted of very light and homogeneous flakes of very small particle size.

2.4. Instruments

Thermogravimetric analysis (TGA; DTA Instruments, SDT2960) of the precursor samples was studied using Shimadzu DT-50 thermal analyzer. Samples were carried out in static atmosphere of air against α-Al_2O_3 as a reference at a constant heating rate of 10 °C min^{-1}. The experiments were carried out in the temperature range between room temperature and 1000 °C. Infrared spectra of the samples were recorded in the range of 200–4000 cm^{-1} using Jasco FT/IR-460 plus. The method includes mixing few milligrams of calcined powder of the sample with potassium bromide (KBr) powder in agate mortar. The mixture was then pressed by means of hydraulic press. The absorbance was automatically recorded against wavenumber (cm^{-1}). The functional groups of calcined powder were characterized by Infrared spectra. X-ray diffraction analysis was performed on SIEMENS D5000. The patterns were run with Cu-filtered Cu K_α radiation (1.79 Å) energized at 45 kV and 10 mA. The samples were measured at room temperature in the range $2\theta = (20–80°)$. Phase formation and particle size of product were identified using X-ray diffraction analysis data. The morphology and particle shape for the calcined powder were performed using TEM, model EM 10 Zeiss, at 60 kV by dispersed sample in water on a copper grid. The diffuse reflectance of fired pigments was measured in JASCO spectrophotometer UV–visible in 200–800 nm range using standard D65 illumination and barium sulfate as reference and the CIE-$L^*a^*b^*$ colorimetric method, recommended by the Commission Internationale de l'Eclairage (CIE) [39]. Electronic spectra measurements were carried out using JASCO V530 UV/vis spectrophotometer in the range of 200–800 nm for both calcinated samples using 10 nm-matched quartz cells. The mixtures of prepared sample were calcinated in alumina crucibles.

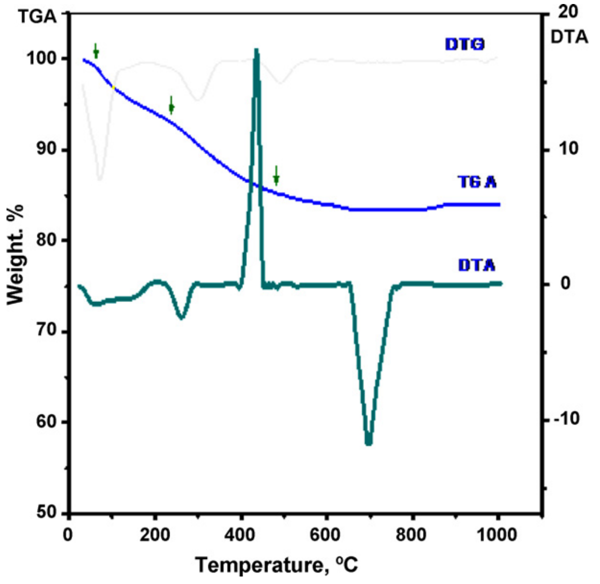

Fig. 1. Thermal analysis (TG–DTG/DTA) of 0.05 mole of Co^{2+}.

3. Results and discussion

3.1. Thermal analysis

Thermal analysis for 0.05 mole of Co^{2+} using oxalyldihydrazide as fuel showed that the weight losing of system after ignition using this fuel changed in three steps as shown in Fig. 1. The losing weight of 13% (calc. 13.5%) in the first range 50–200 °C and the second range 200–450 °C occurred due to elimination of the humidity and co-ordination water in sample. The losing weight of 10% (calc. 11%) in the range 450–650 °C occurred due to the evolution of CO, CO_2 and NO_x gases from sample. DTG shows three peaks at 100, 300 and 500 °C, respectively. The differential thermal analysis (DTA) shows two endothermic steps and only one exothermic step. The first

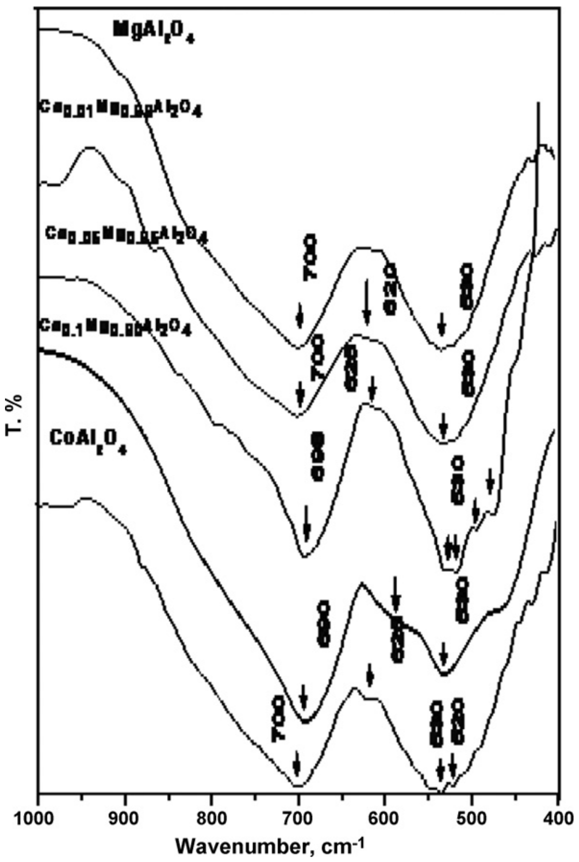

Fig. 2. Infrared spectra for 0.01, 0.05 and 0.10 mole of Co^{2+} systems, $CoAl_2O_4$ and $MgAl_2O_4$ using oxalyldihydrazide as fuel at 1200 °C.

Table 1
Assignment of the important bands in the FTIR spectra for 0.01, 0.05 and 0.10 mole of Co^{2+} systems at different calcination temperatures using oxalyldihydrazide as fuel.

Temp. (°C)	Bands assignment						
	ν_{-OH}	ν_{-CH}	$\nu_{C=O}$	ν_{C-O}	ν_{C-N}	$\nu_{N=O}$	ν_{M-O}
0.01 mole of Co^{2+}							
500	3490	2920	1650	1100	1400	800	600
700	3460	–	1650	1150	1450	800	695, 500, 425
900	3450	–	–	–	1450	–	700, 610, 515
1100	3400	–	–	–	–	–	698, 610, 510, 410
1200	3400	–	–	–	–	–	698, 521, 428
0.05 mole of Co^{2+}							
500	3490	2950	1650	1100	1400	800	–
700	3490	–	1650	1110	1390	–	700, 500
900	3400	–	1650	1110	–	–	700, 515, 422
1100	3410	–	–	–	–	–	691, 520, 422
1200	3420	–	–	–	–	–	685, 522, 422
0.10 mole of Co^{2+}							
500	3490	2850	1680	1110	1390	800	500, 700
700	3450	–	1620	1110	–	–	700, 530
900	3450	–	1650	1110	1400	–	697, 530, 420
1100	3490	–	–	–	–	–	690, 425, 530
1200	3500	–	–	–	–	–	690, 610, 530, 425

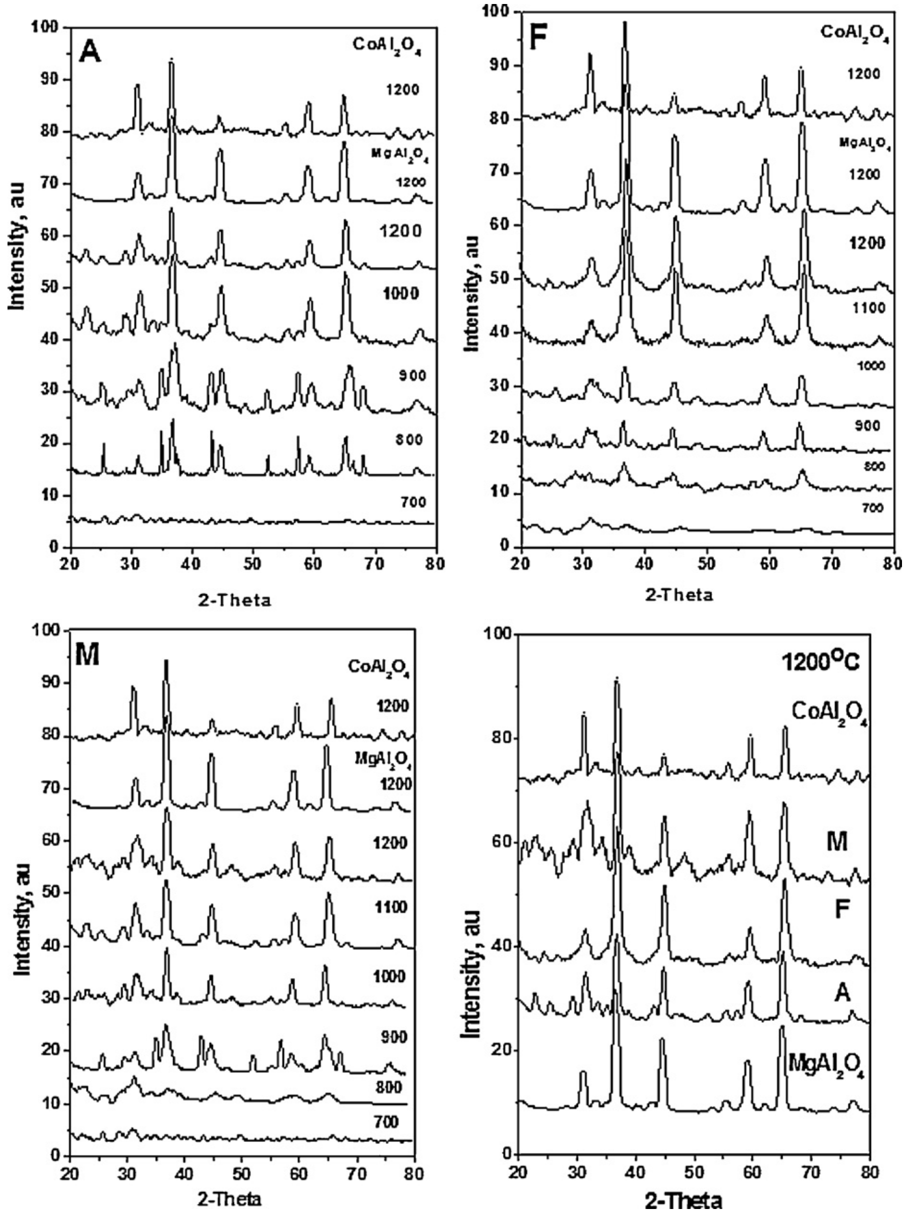

Fig. 3. X-ray diffraction patterns for 0.001 mole (A), 0.05 mole (F) and 0.10 mole (M) of Co^{2+} systems at different calcination temperatures using oxalyldihydrazide as fuel.

endothermic step occurred for elimination of the water in sample. The second endothermic peak shows phase formation. The exothermic peak was due to elimination of the residual organic material in sample. We can explain the calcination steps as the following equations using oxalyl-dihydrazide (ODH).

$$0.05CoCO_3\cdot 0.95MgO\cdot Al_2O_3\cdot 1.5H_2O \xrightarrow{50\text{–}200\,^\circ\mathrm{C}} 0.05CoCO_3\cdot 0.95MgO\cdot Al_2O_3 + 1.5H_2O$$

$$0.05CoCO_3\cdot 0.95MgO\cdot Al_2O_3 \xrightarrow{200\text{–}450\,^\circ\mathrm{C}} Co_{0.05}Mg_{0.95}Al_2O_4 + 0.05CO_2$$

3.2. FTIR spectra

FTIR spectra of 0.01, 0.05 and 0.10 mole Co^{2+} for A, F and M systems, respectively using oxalyldihydrazide as fuel are studied after ignition and calcinations at different temperatures. The broad absorption bands around 3490 cm^{-1} for A, F and M systems, respectively correspond to the stretching vibration of surface and free (–OH) group of water molecules [40]. The absorption bands at 2920 cm^{-1} for A and F systems, 2950 cm^{-1} for M system are related to the stretching vibration of C–H aliphatic in organic molecules. The absorption bands at 1650 and 1100 cm^{-1} are related to the stretching vibration of C=O and C–O groups of residual organic fuel [41]. The absorption bands at 1658, 1383 and 825 cm^{-1}, respectively correspond to undecomposed [42] nitrate ions.

Fig. 2 shows the absorption bands in the region 400–1000 cm^{-1} due to the formation of spinel structure after calcinations at different temperatures in the range 500–1200 °C. These bands in the region 800–4000 cm^{-1} disappeared at 1100 °C except, the strong absorption bands at 3480 cm^{-1} for A, F and M systems, respectively, correspond to the stretching vibration of adsorption water molecules [43]. The two absorption bands at 700 and 535 cm^{-1} for A system and the vibrational bands at 690, 530 and 520 cm^{-1} for F and M systems, respectively are corresponding to AlO_6 groups building up the spinel as a result of vibration of Al^{3+} ions in octahedral positions [44,45] comparing with the bands at 700, 530 and 420 cm^{-1} which related to $MgAl_2O_4$ spinel. The other vibrational bands at 700, 535 and 420 cm^{-1} for A system, at 690, 530, 520 and 422 cm^{-1} for F system and 690, 530, 520 and 418 cm^{-1} for M system are corresponding to CoO_4/MgO_4 groups for the cobalt and magnesium aluminate spinel as a result of vibration of its ions (Co^{2+} and Mg^{2+}) in the tetrahedral sites comparing with that in the range 700 and 530 cm^{-1} for $CoAl_2O_4$ spinel as blank [46,47]. The assignment of an important band in the IR spectra for 0.01, 0.05 and 0.10 mole of Co^{2+} systems at different calcination temperatures using oxalyldihydrazide as fuel are listed in Table 1.

3.3. X-ray diffraction and particle size measurement

The X-ray diffraction for cobalt ion as doping for $MgAl_2O_4$ system using oxalyldihydrazide as fuel is investigated as powders at different calcination temperatures. Fig. 3 shows the X-ray band intensities against (2θ) for A, F and M systems. From X-ray patterns, it is clear that the intensity of the bands is increasing with calcined temperatures. The calcinated powders begin to exist the spinel crystalline and the disappearance of Al_2O_3 at 1000 °C. With the increase of the temperature above 1000 °C, intensities of the peaks increase gradually until sharpen peaks are observed at 1200 °C [48,49]. The average crystallite sizes calculated from the X-ray diffraction peaks using Scherrer's equation. The crystalline spinel phase content and the particle size increase with increasing calcination temperature shown in Fig. 4. The particle sizes of different doping Co^{2+} systems from XRD are shown in Table 2. Particle sizes of different doping Co^{2+} systems calculated from X-ray compared with transmission electron microscopy data are shown in Table 3. The bulk densities of samples under investigation calculated from X-ray and compared with the experimental obtained from Archimedes' law are shown in Table 4.

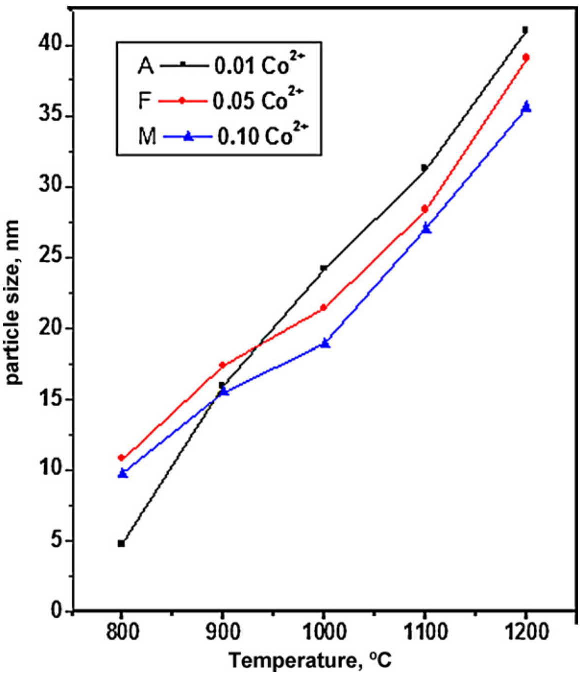

Fig. 4. The correlation between particle size from X-ray diffraction for 0.01, 0.05 and 0.1 mole of Co^{2+} systems and different calcination temperatures using oxalyldihydrazide as fuel.

Table 2
The particle size from X-ray diffraction at different calcination temperatures.

System	Calcination temperatures (°C)					
	700	800	900	1000	1100	1200
0.01	Am[a]	4.7	15.90	24.14	31.20	37.69
0.05	Am	3.1	17.29	21.36	28.30	31.175
0.10	Am	9.68	15.50	18.82	27.02	35.57

[a] Amorphous.

The microstructure of nano ceramic pigments at different calcination temperatures is performed using transmission electron microscopy. Fig. 5 shows the photographs for the compounds under investigation which exhibit the spherical particles for 0.01, 0.05 and 0.1 mole of Co^{2+} systems. The particle sizes observed by TEM are in agreement with that observed by XRD. Also, the morphology and particle sizes are decreased as the amount of doping Co^{2+} ion increases. From all these data, the morphology of $CoAl_2O_4$ and $MgAl_2O_4$ spinel for different systems has the spherical shapes.

3.4. The color characterization of nano ceramic pigments

Diffuse reflectance spectra for A, F and M systems using oxalyldihydrazide as fuel present in Fig. 6. The appearance of bands

Table 3
XRD and TEM particle sizes for different cobalt systems at 1100 °C.

System	Particle size (nm)	
	XRD	TEM
0.01	31.20	32.00
0.05	28.30	30.00
0.10	27.02	28.00

Table 4
Lattice parameters and bulk density of different cobalt systems using oxalyldihydrazide as fuel.

System	Parameters	Calcination temperature (°C)				
		800	900	1000	1100	1200
0.01	a	8.075	8.085	8.0887	8.1066	8.1231
	a^3	526.54	528.49	529.22	532.27	536
	d_{theo} (g ml^{-1})	3.590	3.5798	3.572	3.552	3.548
	d_{exp} (g ml^{-1})	3.570	3.560	3.550	3.530	3.510
0.05	a	8.070	8.075	8.0806	8.085	8.0948
	a^3	525.45	526.54	527.65	528.49	530.42
	d_{theo} (g ml^{-1})	3.703	3.624	3.618	3.611	3.598
	d_{exp} (g ml^{-1})	3.700	3.600	3.570	3.550	3.535
0.10	a	8.070	8.075	8.0806	8.085	8.0887
	a^3	525.45	526.54	527.65	528.49	529.22
	d_{theo} (g ml^{-1})	3.674	3.6678	3.660	3.654	3.650
	d_{exp} (g ml^{-1})	3.650	3.633	3.610	3.600	3.950

in range 495 and 450 nm for A system, 450 nm for F system and 440 nm for M system for oxalyldihydrazide at 700 °C those results reveal that the pale blue color of samples. These bands shift to blue side as calcinated temperatures increase until reaching around 435 and 490 nm for A system, 435 and 495 nm for F system 430 and 390 nm for M system at 900 °C. These bands shift to blue side at 480, 460 and 425 nm for A and M systems and 480, 425 nm for F system at 1200 °C which show the bluest [50,51] color pigments.

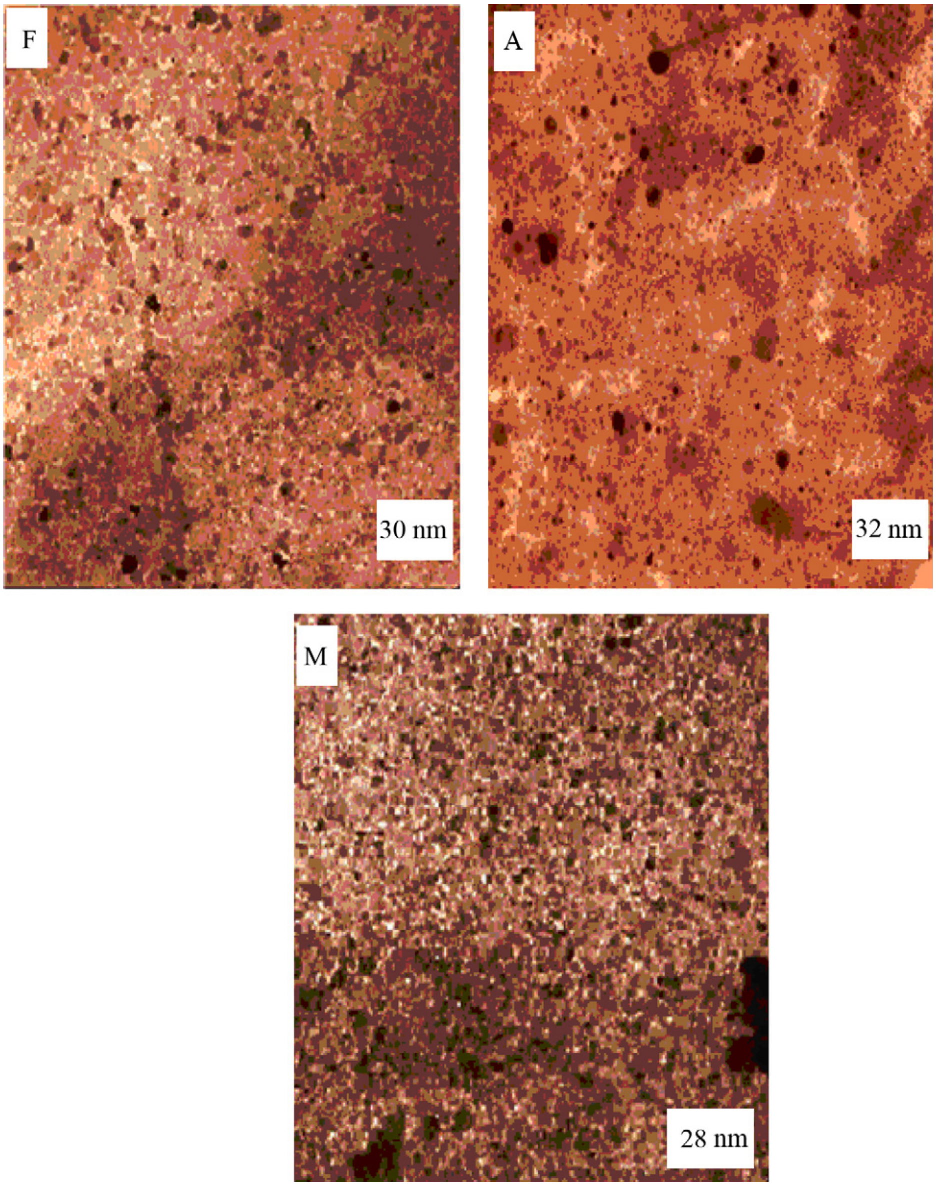

Fig. 5. Transmission electron microscopy (TEM) images for A = 0.01, F = 0.05 and M = 0.10 mole of Co^{2+} systems at 1100 °C by using oxalyldihydrazide as fuel.

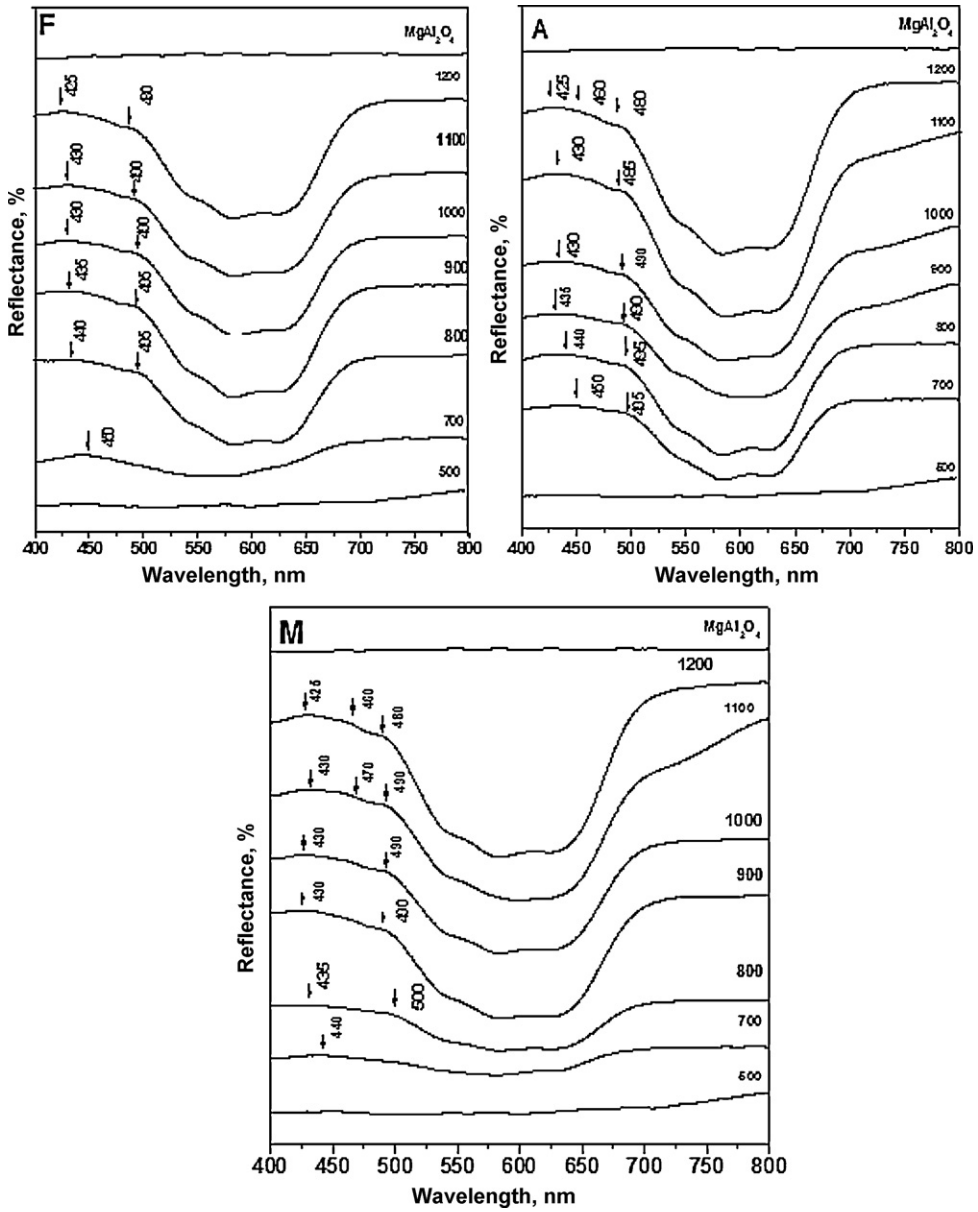

Fig. 6. Diffuse reflectance spectra of A system (0.01 mole of Co^{2+}), F system (0.05 mole of Co^{2+}) and M system (0.10 mole of Co^{2+}) at different calcination temperatures using oxalyldihydrazide as fuel.

According to the colorimetric data present in Table 5 the L^* values decrease while b^* values increases in negative direction as a result of increasing calcination temperatures. The increase in negative values of b^* means the higher intensity of blue color. The decrease in L^* parameter tends to reduce the lightness of sample. The values of a^* are random for oxalyldihydrazide. Fig. 7 shows the correlation between calcination temperatures with b^* values depending on the amount of cobalt present, the value of b^* increases leading to the depth of blue color. The lower value of hue variation ΔE tends to a good color matching [52]. Colorimetric data using oxalyldihydrazide show the high negative value of b^* and lower value of hue variation ΔE at 1200 °C for 0.01 and 0.05 mole doping cobalt. This means that the appearance of good pigment powder color and a good color matching occur at 1200 °C for A and F systems. On the other hand, the high value of b^* for M system presents at 1100 °C and lower value of hue variation ΔE at 1200 °C. This means that the appearance of good pigment powder color at 1100 °C and a good color matching occur at 1200 °C for M doping cobalt as shown in Table 5. The diffuse reflectance spectra data show the bluest color pigment as given in Table 5. At the same time, the increase of the amount of cobalt ion reveals the increase of defect in crystal structure of spinel. These defects occurring in spinel structure lead to the distorted tetrahedral and octahedral sites, which in return change oxygen as the ligand around cobalt(II) ion as the chromophore and hence change of intensity color is observed [53].

3.5. Electronic spectra

The electronic spectra for cobalt systems using oxalyldihydrazide as fuel are explained. The electronic spectra of A, F and M systems of cobalt(II) ion using oxalyldihydrazide as fuel show the presence of broad band at 600 nm for M system and no bands for A and F systems. The absorption of these bands increases

Table 5
Colorimetric data for 0.01, 0.05 and 0.1 mole of Co^{2+} systems at different calcination temperatures using oxalyl-dihydrazide as fuel.

System	Temperature (°C)	L^*	a^*	b^*	ΔE
0.01	500	99.74	−0.02	−0.10	99.74
	700	97.9	−0.19	−2.20	97.93
	800	95.25	−0.75	−3.14	95.31
	900	94.20	−1.60	−6.43	94.43
	1000	92.51	−0.81	−6.61	92.75
	1100	91.32	−1.68	−6.98	91.60
	1200	90.60	−1.36	−8.04	90.97
0.05	500	98.77	−0.13	3.81	98.84
	700	97.3	−1.16	−3.52	97.37
	800	96.53	−0.71	−4.65	96.65
	900	96.07	−1.69	−5.38	96.24
	1000	94.41	−1.79	−7.38	94.72
	1100	92.76	−1.15	−9.12	93.21
	1200	91.41	−1.31	−10.5	92.02
0.10	500	97.37	−0.07	0.02	97.37
	700	95.43	−0.80	−4.20	95.53
	800	93.29	−1.78	−7.05	93.57
	900	92.28	−1.24	−9.17	92.74
	1000	90.97	−2.35	−11.79	91.76
	1100	89.19	−1.66	−13.43	90.21
	1200	84.77	−2.32	−12.34	85.70

with calcination temperature from 700 to 1200 °C. These bands appear as three broad absorption bands at 543 nm (green region), 588 nm (yellow-orange region) and 630 nm (red region) for A system, 543 nm, 588 nm and 625 nm for F system and 543 nm, 588 nm and 625 nm for M system at 1200 °C using oxalyldihydrazide. Three intense bands are present at 15,385, 17,000 and 19,000 cm^{-1}, which correspond to the electronic transition of cobalt(II) ion in tetrahedral coordination sites. The tetrahedral coordination of cobalt(II) ion which gives rise to the blue color as present in Fig. 8. This absorption could be assigned to the $^4A_2(F) \rightarrow {}^4T_1(P)$, $^4A_2(F) \rightarrow {}^4T_1(F)$ and $^4A_2(F) \rightarrow {}^4T_2(F)$. This triple bands in visible region can be attributed to Jahn–Teller distortion of octahedral structure [54,55].

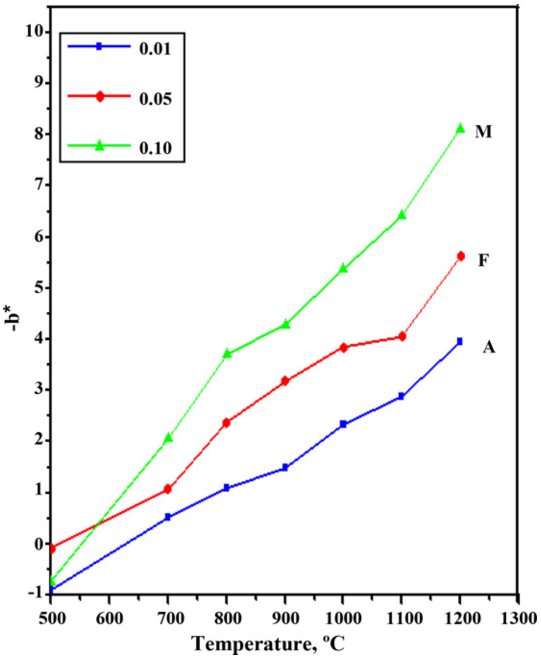

Fig. 7. Colorimetric data for 0.01, 0.05 and 0.1 mole of Co^{2+} systems at different calcination temperatures using oxalyldihydrazide as fuel.

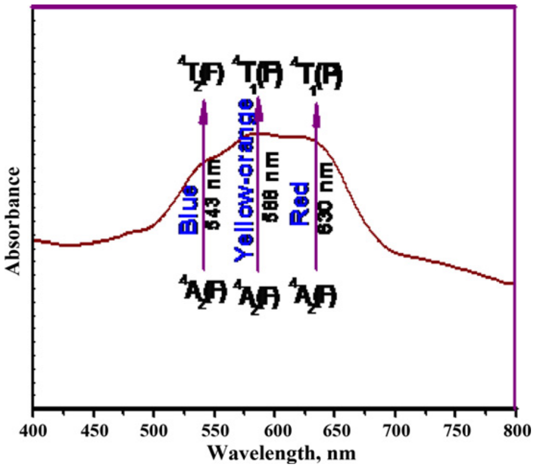

Fig. 8. Electronic spectrum for 0.01 mole of Co^{2+} systems in nujol mull at 1000 °C calcination temperature using oxalyldihydrazide as fuel.

4. Conclusions

$MgAl_2O_4$: xCo^{2+} nano-powders ($0.00 \le x \le 0.10$) as blue ceramic pigments were prepared by the low temperature combustion synthesis (LCS) method. The characterization of nano refractory pigments was studied by FTIR spectroscopy, electronic spectroscopy, diffuse reflectance spectroscopy (DRS), different techniques of thermal analysis (TG–DTG/DTA), X-ray diffraction (XRD) and Transmission electron microscopy (TEM). The calcination temperatures in the range 500–1200 °C give nano-particles with particle sizes in the range of 3.1–37.69 nm using oxalyldihydrazide as fuel. The particle sizes increased as sintering of samples at different calcination temperatures and TEM shows spherical shape with nano-scale at different calcination temperatures. FTIR and X-ray show the formation of spinel structure of $Co_xMg_{1-x}Al_2O_4$. The blue color intensity increased as the amount of cobalt increased calcination temperature and time. Electronic spectra give broad absorption band with triple shoulders as a result of Jahn–Teller distortion of octahedral structure.

References

[1] M. Cain, R. Morrell, Appl. Organomet. Chem. 15 (2001) 321.
[2] Z. Hu, M. Xue, Q. Zhang, Q. Sheng, Y. Liu, Dyes Pigm. 76 (2008) 173.
[3] S.K. Biswas, D. Dhak, A. Pathak, P. Pramanik, Mater. Res. Bull. 43 (2008) 665.
[4] G. Buxbaum, Industrial Inorganic Pigments, second ed., Wiley-VCH, 1997.
[5] A. Burgyan, Interceram. NR 1 (1979) 30.
[6] E.S. Kharashvili, Glass Ceram. 42 (1985) 459.
[7] R.W. Batchelor, Trans. Br. Ceram. Soc. 73 (1974) 297.
[8] J. Livage, Inorganic Materials, Sol–Gel Synthesis of, Encyclopedia of Materials: Science and Technology, 2010, ISBN 0-08-0431526, pp. 4105–4108.
[9] D. Segal, J. Mater. Chem. 7 (1997) 1297.
[10] C.O. Arean, M.P. Mentruit, E.E. Scalona, F.X. Xamena, J.B. Parra, Mater. Lett. 12 (1999) 537.
[11] P. Phule, T.E. Wood, Sol–Gel Synthesis of Ceramics and Glasses, Encyclopedia of Materials: Science and Technology, 2004, ISBN 0-08-0431526, pp. 1090–1095.
[12] M. lade, H. Mays, J. Schmidt, R. Willumeit, R. Schomacker, Colloids Surfaces A: Physicochem. 163 (2000) 3.
[13] R.E. Riman, W.L. Suchanek, M.M. Lencka, Ann. Chim. Sci. Mater. 27 (2002) 15.
[14] Z. Chen, E. Shi, W. Li, Y. Zheng, N. Wu, W. Zhong, J. Am. Ceram. Soc. 85 (2002) 2949.
[15] Y.W. Chen, T.M. Yen, C. Li, J. Non-Cryst. Solids 185 (1995) 49.
[16] R. Julian, J. Osman, J.A. Crayston, A. Pratt, D.T. Richens, Mater. Chem. Phys. 110 (2008) 256.
[17] K. Kim, C. Kim, J. Eur. Ceram. Soc. 24 (2004) 2613.
[18] M. Kakihana, J. Sol–Gel Sci. Technol. 6 (1996) 7.
[19] X. Yu, X. He, S. Yang, X. Yang, X. Xu, J. Mater. Lett. 58 (2003) 48.
[20] I.S. Ahmed, H.A. Dessouki, A.A. Ali, Spectrochim. Acta 71A (2008) 616.
[21] I.S. Ahmed, H.A. Dessouki, S.A. Shama, M.M. Moustafa, A.A. Ali, Spectrochim. Acta 74A (2009) 665.
[22] R. Ianoş, I. Lazău, C. Păcurariu, P. Barvinschi, Mater. Res. Bull. 43 (2008) 3408.

[23] X. Huang, J. Chang, Mater. Chem. Phys. 115 (2009) 1.
[24] M.D. Nersesyan, A.G. Peresada, A.G. Merzhanov, Int. J. SHS 7 (1998) 60.
[25] R. Ianoş, I. Lazău, Mater. Chem. Phys. 115 (2009) 645.
[26] P. Barpanda, S.K. Behera, P.K. Gupta, S.K. Pratihar, S. Bhattacharya, J. Eur. Ceram. Soc. 26 (2006) 2603.
[27] S.T. Aruna, S. Ghosh, K.C. Patil, Int. J. Inorg. Mater. 3 (2001) 387.
[28] D.S. Gouveia, L.E.B. Soledade, C.A. Paskocimas, E. Longo, A.G. Souza, I.M.G. Santos, Mater. Res. Bull. 41 (2006) 2049.
[29] R.A. Candeia, M.A.F. Souza, M.I.B. Bernardi, S.C. Maestrelli, Mater. Res. Bull. 41 (2006) 183.
[30] R.A. Candeia, M.A.F. Souza, M.I.B. Bernardi, S.C. Maestrelli, I.M.G. Santos, A.G. Souza, E. Longo, Ceram. Int. 33 (2007) 521.
[31] R.A. Candeia, M.I.B. Bernardi, E. Longo, I.M.G. Santos, A.G. Souza, Mater. Lett. 58 (2004) 569.
[32] R.K. Mason, J. Am. Ceram. Soc. Bull. 40 (1961) 5.
[33] G. Monnari, T. Manfrd, J. Ceram. Eng. Sci. Process 17 (1996) 102.
[34] V. Sepelak, K.D. Becker, Mater. Sci. Eng. A 375–377 (2004) 861.
[35] M. Llusar, A. Forés, J.A. Badenes, J. Calbo, M.A. Tena, G. Monrós, J. Eur. Ceram. Soc. 21 (2001) 1121.
[36] W. Li, J. Guo, J. Li, J. Eur. Ceram. Soc. 23 (2003) 2289.
[37] D.V. Sanghani, G.R. Abrams, P.J. Smith, Trans. J. Br. Ceram. Soc. 80 (1981) 210.
[38] G.V. Mahesh, P. Ravindranathan, K.C. Patil, Proc. Indian Acad. Sci. (Chem. Sci.) 97 (1986) 117.
[39] CIE, Recommendations of Uniform Color Spaces, Color Difference Equations, Psychometrics Color Terms, Supplement no. 2 of CIE Publ. No. 15 (E1-1.31), 1971, Bureau Central de la CIE, Paris, 1978.
[40] M.F.M. Zawrah, A.A. El Kheshen, Br. Ceram. Trans. 101 (2002) 71.
[41] K. Nakamoto, Infrared and Raman Spectra of Inorganic and Coordination Compounds, fourth ed., Wiley Press, New York, 1986, p. 231.
[42] P. Duran, J. Tartaj, F. Rubio, C. Moure, O. Pena, J. Ceram. Int. 31 (2005) 599.
[43] A.K. Adak, A. Pathak, A. Pramanik, Br. Ceram. Trans. 98 (1999) 200.
[44] N.N. Boguslavska, E.F. Venger, N.M. Vernidub, Y.A. Pasechnik, K.V. Shportko, Reststrahlen spectroscopy of $MgAl_2O_4$ spinel, Semiconductor Physics, Quantum Electron. Optoelectron. 5 (2002) 95.
[45] P. Tarte, Spectrochim. Acta 23A (1967) 2127.
[46] A.Y. Chapskaya, N.I. Radishevskaya, N.G. Kasatskii, O.K. Lepakova, Y.S. Naiborodenko, V.V. Vereshchagin, J. Glass Ceram. 62 (2005) 11.
[47] L.F. Koroleva Chekhomova, Glass Ceram. 61 (2004) 9.
[48] X. Duan, D. Yuan, C. Luan, Z. Sun, D. Xu, M. Lv, J. Non-Cryst. Solids 328 (2003) 245.
[49] Z. Chen, E. Shi, W. Li, Y. Zheng, W. Zhong, Mater. Lett. 55 (2002) 281.
[50] A. Tucks, H.P. beck, J. Solid State Chem. 178 (2005) 1145.
[51] K. Nassau, The Physics and Chemistry of Color—The Fifteen Causes of Color, vol. 5, Wiley-Interscience Publication, John Wiley & Sons, 1983, pp. 79–85.
[52] F. Bondioli, T. Manfredini, M. Romagnoli, J. Eur. Ceram. Soc. 26 (2006) 311.
[53] M. Llusar, A. Fores, J.A. Badenes, J. Calbo, M.A. Tena, G. Monros, J. Eur. Ceram. Soc. 21 (2001) 1121.
[54] C.R. Bambord, Phys. Chem. Glasses 3 (1962) 189.
[55] T. Bates, Ligand field theory and absorption spectra of transition-metal ions in glasses Modern Aspects of the Vitreous State, vol. 2, Butterworths, London, 1961, pp. 195–254.